Density compensation for iterative reconstruction from under-sampled radial data

Boris Mailhe[1], Qiu Wang[1], Robert Grimm[2], Marcel Dominik Nickel[2], Kai Tobias Block[3], Hersh Chandarana[3], and Mariappan S. Nadar[1]

[1]Imaging and Computer Vision, Siemens Corporation, Corporate Technology, Princeton, NJ, United States, [2]MR Application & Workflow Development, Siemens Healthcare, Erlangen, Germany, [3]Department of Radiology, New York University School of Medicine, New York, NY, United States

Target audience: Biomedical engineers performing iterative image reconstruction on non-Cartesian variable-density sampling data, in particular radial trajectories.

Purpose: The goal of this research is to accelerate iterative GRASP reconstruction [1] by reducing the number of NUFFTs required to produce sharp images. In radial sampling patterns with uniform spoke sampling such as used in GRASP [2], the k-space center is more densely sampled than high frequencies. In direct reconstruction from fully sampled radial data, this variable-density sampling can be compensated at reconstruction by applying a ramp filter in k-space before re-gridding. In this work, we extend the concept of density compensation to iterative reconstruction from under-sampled data. A ramp filter enhances high frequencies too much in the under-sampled case, so instead we calibrate the filter from the radial Fourier transform. Besides, within the regularized iterative reconstruction framework, the filter has to be applied to the image being reconstructed, not the raw data. We express the filter in Cartesian k-space so that it can easily be applied to images by fast FFT-based convolution.

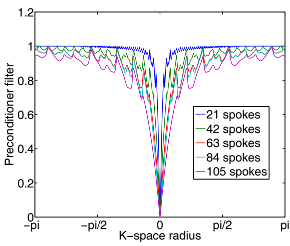

Figure 1: radial filter for different groupings.

$$\min_{x} \|y - Ax\|_2^2 + \lambda \|Wx\|_1 \quad (1) \qquad \min_{x,z|x=Pz} \|y - APz\|_2^2 + \lambda \|Wx\|_1 \quad (2) \qquad x \leftarrow x + \alpha PP^H A^H (y - Ax) \quad (3)$$

Methods: Iterative MRI reconstruction from under-sampled data can be expressed as Problem (1), with *y* the measurements, *A* the SENSE parallel radial measurement operator, *x* the target image and *W* a sparsifying transform such as a wavelet or finite differences [3]. Problem (1) can also be interpreted as a Bayesian MAP estimator under a white Gaussian noise model on the measurements [4]. The decay speed of the quadratic term by first-order optimization methods depends on the condition number of *A*, i.e. the ratio between its absolute highest and lowest non-zero singular values [5]. Radial variable density can also be understood in terms of conditioning: low-frequency subspaces are associated to higher singular values than high-frequency subspaces.

To improve conditioning, one can instead solve Problem (2), with *P* chosen so that *AP* is well-conditioned. Density compensation on the raw measurements would apply *P* to the left of *A* instead, but in the regularized reconstruction context, this is equivalent to weighting the norm used to measure data fidelity, i.e. changing the covariance of the assumed noise distribution. Using a proximal gradient optimization algorithm such as FISTA [6], right-hand-side preconditioning modifies the gradient descent step into Equation (3), with α a step size and $A^H(y-Ax)$ the gradient of the quadratic term in Problem (1) with respect to *x*.

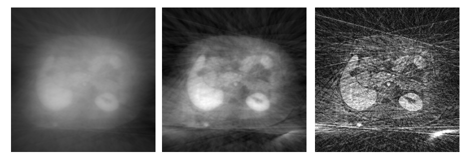

None Calibrated Ramp

Figure 2: First descent direction

P is a high-pass image filter with radial symmetry, expressed in Cartesian k-space for efficient application to images by fast convolution. It depends on the number of spokes grouped in each reconstructed frame, but is independent of the k-space data, so *P* can be calibrated offline and the same preconditioner can be re-used to reconstruct all the images acquired with a given sampling pattern. Since *P* is assumed to have radial symmetry, its radial values are computed by applying power algorithms on the radial NUFFT co-restricted to each possible k-space radius, and using the inverses of the obtained singular values as the matching preconditioner values. Figure 1 shows the radial preconditioner profiles for different spoke groupings. As the number of spokes decreases, their cut-off becomes sharper. The filters in Cartesian k-space are derived from the radial profiles by linear interpolation, and then the squared preconditioner PP^H is pre-computed and saved on file.

At any iteration, applying the preconditioner to the gradient takes one Cartesian FFT, one Hadamard product and one adjoint FFT per frame. As a comparison, computing the gradient requires one Hadamard product (to apply the coil sensitivities), one NUFFT and one adjoint NUFFT per frame and per channel.

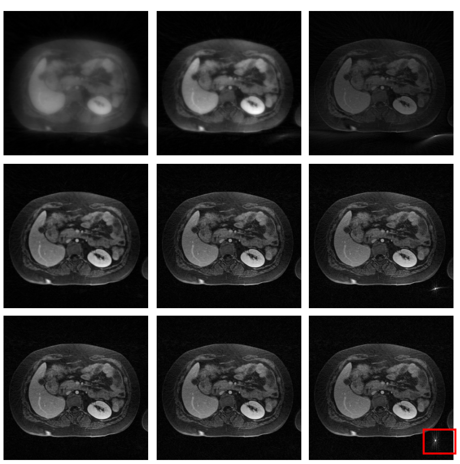

None Calibrated Ramp

Figure 3: Reconstruction after 10, 50 and 100 iteration (from top to bottom)

<u>*Data acquisition*</u>: A pediatric abdominal Dynamic Contrast Enhanced scan was performed using a prototypical VIBE pulse sequence with a golden-angle stack-of-star trajectory having 512 samples per spoke. MR acquisitions were performed on a clinical 1.5T scanner (MAGNETOM Avanto, Siemens AG, Healthcare Sector, Erlangen, Germany). Data were decoupled along the slice direction, and for each slice a time series was reconstructed with a uniform temporal resolution of 21 spokes per frame and a full-FOV in-plane resolution of 512x512.

<u>*Image Reconstruction:*</u> Reconstruction was performed using 100 iterations of the FISTA algorithm with three preconditioning settings: no preconditioning, ramp filter, and the calibrated preconditioner, with step sizes set to the inverse squared highest singular value of the preconditioned measurement operator *AP*. The initial images are all zeros. *W* is a combination of redundant Haar wavelet and second derivative over time [7].

Results: The overall image quality and spatial resolution of the different experiments was visually inspected. Figure 2 shows the first descent direction for the three different reconstructions for one slice and one time point of the reconstructed volume. The gradient with no preconditioning appears blurred, with little contrast difference between tissues. The ramp filter increases streaking artifacts, and the calibrated preconditioner achieves a trade-off between the two. Figure 3 shows the reconstruction after 10, 50 and 100 iterations. The reconstructed images are sharpened faster with preconditioning, but the ramp filter generates an artifact in the lower right corner that does not vanish with more iterations. After 50 iterations with preconditioning, image quality is similar to 100 iterations without.

Discussion and Conclusion: Density compensation is a mandatory step for non-iterative Filtered Back-Projection reconstruction techniques. In this work we described how to extend this concept to iterative reconstruction by linking it with preconditioning of linear operators. While not strictly necessary, we showed that applying density compensation to the successive gradients improves image sharpness and accelerates the convergence of the reconstruction algorithm. We also showed that the density compensation filters known from the fully sampled case are not necessarily suitable to under-sampled acquisitions, but that correct filters can be calibrated for a given acquisition protocol.

References: [1] L. Feng et al., Mag. Res. Med., Sep, 72(3):707-717, 2014 [2] S. Winkelmann et al., IEEE Trans. Med. Im., Jan, 26(1):68-76, 2007 [3] M. Lustig et al., Mag. Res. Med., Dec, 58(6):1182-1195, 2007 [4] R. Gribonval, IEEE Trans. Sig. Proc., Jan, 59(5):2405-2410 [5] H.A. van der Vorst, Cambridge University Press, 2009 [6] A. Beck and M. Teboulle, SIAM J. Im. Sci., 2(1):183-202, 2009 [7] Q. Wang et al., ISMRM 2015, submitted